

# 感兴趣区域高效提取算法\*

张红梅<sup>1+</sup>, 卞正中<sup>1</sup>, 郭佑民<sup>2</sup>, 叶敏<sup>3</sup>

<sup>1</sup>(西安交通大学 生命科学与技术学院, 陕西 西安 710049)

<sup>2</sup>(西安交通大学 第一附属医院影像中心, 陕西 西安 710061)

<sup>3</sup>(西安交通大学 机械学院, 陕西 西安 710049)

## An Efficient Approach to Extraction of Region of Interest

ZHANG Hong-Mei<sup>1+</sup>, BIAN Zheng-Zhong<sup>1</sup>, GUO You-Min<sup>2</sup>, YE Min<sup>3</sup>

<sup>1</sup>(School of Life Science and Technology, Xi'an Jiaotong University, Xi'an 710049, China)

<sup>2</sup>(Imaging Center of the First Affiliated Hospital, Xi'an Jiaotong University, Xi'an 710061, China)

<sup>3</sup>(School of Mechanical Engineering, Xi'an Jiaotong University, Xi'an 710049, China)

+ Corresponding author: Phn: +86-29-85236872, E-mail: clamei@mailst.xjtu.edu.cn, <http://www.xjtu.edu.cn>

Received 2003-11-26; Accepted 2004-02-20

Zhang HM, Bian ZZ, Guo YM, Ye M. An efficient approach to extraction of region of interest. *Journal of Software*, 2005,16(1):77-88. <http://www.jos.org.cn/1000-9825/16/77.htm>

**Abstract:** ROI (region of interest) plays an important role in medical image analysis. In this paper, an efficient approach to ROI extraction based on monotonically marching curve evolution is proposed. The improvement is in two aspects: first, a new monotonically marching snake integrating ROI information is presented by minimizing the new defined ROI energy. Due to the region based speed term, the front could even propagate in low contrast and narrow thin areas. Second, a multi-initial fast marching algorithm is developed for numerical implementation, where a multi-initial scheme can perform the selective growth of the front, thus further reduce the front leaking. Furthermore, a multiscale scheme for numerical implementation is adopted, where a fast passing solution method is used for determining the initial solution on the finer scale that greatly reduces the computational cost. The validity of the proposed approach is demonstrated on the medical image ROI extraction. Experimental results show that the approach is efficient both in computational cost and segmentation quality. Low contrast and narrow thin ROI could be efficiently extracted precisely by the approach.

**Key words:** ROI(region of interest); curve evolution; multiscale scheme; multi-initial fast marching algorithm; segmentation

---

\* Supported by the National Nature Science Foundation of China under Grant Nos.60271022, 60271025, 3020066 (国家自然科学基金); the Vital Clinical Subject Foundation of China under Grant No.20012028 (卫生部临床学科重点项目)

**ZHANG Hong-Mei** was born in 1973. She received her Ph.D. degree at the School of Life Science and Technology, Xi'an Jiaotong University. Her research is medical image processing. **BIAN Zheng-Zhong** was born in 1938. He is a professor and doctor supervisor at the School of Life Science and Technology, Xi'an Jiaotong University. His research is image processing. **GUO You-Min** was born in 1955. He is a professor and doctor supervisor at the Imaging Center of First Affiliated Hospital, Xi'an Jiaotong University. His research is medical imaging. **YE Min** was born in 1978. He is a Ph.D. candidate at the School of Mechanical Engineering, Xi'an Jiaotong University. His research is fuzzy control.

**摘要:** 感兴趣区域在临床医学图像分析中占有重要地位.提出了一种基于单调推进曲线进化的感兴趣区域提取新方法.首先,通过极小化 ROI(region of interest)能量函数,推导出区域速度函数项,并与基于边界的速度函数融合,提出融合 ROI 信息的单调推进 Snake 模型.ROI 信息能够增强曲线深入到对比度低且细窄的区域中的传播能力.其次,提出了多初始化快速推进算法,选择性地种植种子曲线有助于局部区域的生长从而进一步改善分割结果.此外,为提高计算效率,在多尺度空间进行数值求解,其中利用快速解传递方法实现粗一级尺度到细一级尺度解的传递,可以加速收敛.利用医学图像分割实验对该方法进行评估,结果表明:该方法能够快速、精确地提取低对比度和细窄的 ROI 区域.与现有方法相比,该方法的高效性同时体现在分割结果和计算代价上.

**关键词:** 感兴趣区域;曲线进化;多尺度策略;多初始化快速推进算法;分割

**中图法分类号:** TP391      **文献标识码:** A

## 1 Introduction

Region of interest (ROI) plays a crucial role in medical image analysis. Quantitative analysis of the shape and properties of ROI could provide reliable data for diagnosing disease and the follow-up treatment planning<sup>[1]</sup>. As a result, exploiting an accurate and fast ROI extraction method is in a great need.

In recent years, ROI extraction based on the curve evolution approaches that deform an initial curve towards the desired boundary has been extensively explored. Snakes or active contours first proposed by Michael Kass are energy-minimizing curves that deform to fit the boundary of ROI<sup>[2]</sup>. To overcome some drawbacks of the classical snakes, region based information is introduced to the model. Chakraborty proposed a model that integrates the region based segmentation and boundary finding in a unified framework<sup>[3]</sup>. However its Fourier descriptors limit the shapes that they can describe. Ivins and Zhu proposed the statistical snakes for region growing and applied these models to image/texture segmentation<sup>[4,5]</sup> respectively. However, Due to its “Lagrangian” representation such that the coordinate system moves with the deforming curve, the parametrical snakes could not handle topological changes. To handle the splitting or merging of the curve, extra re-parameterization procedures must be performed during iteration, which brings expensive computational cost<sup>[6]</sup>.

A major breakthrough is made by introducing the level set theory to curve propagation, resulting in a very elegant tool. The level set method proposed by Osher and Sethian offers a highly robust mathematic and numerical implementation on curve/surface evolution<sup>[7]</sup>. Embedding the moving front to be zero level set of a higher dimensional function, topological changes can be handled naturally by exploiting the zero level set at any time. In this approach, selection of a speed function is crucial. On the one hand, the speed function controls the behavior of the front propagation; on the other hand, the form of the speed function decides the computational complexity of the numerical implementation. On solution to the level set evolution equation, Fast Marching method may be the first choice for its low computational cost<sup>[8]</sup>. However, it could only be used for monotonically marching front that requires the speed function be always positive or negative. Narrow band method and Hermes algorithm can cope with all sorts of the level set evolution, but their computational cost is still far more expensive than the fast marching method<sup>[9,10]</sup>.

Malladi in Ref.[8] proposed the image based positive speed function that could stop the front in the vicinity of the ROI boundary. It is a real-time approach, but this only edge based curve evolution may mislead the deformation at weak boundary, as the speed is too weak to propagate the front there. The region-based approaches are more robust compared to the edge-based approaches. Yezzi proposed a fully global approach to image segmentation that is derived based on the deterministic principle of maximally separating the values of certain image statistics within a set of curves<sup>[11]</sup>. However, this approach needs to continually estimate the variable statistics that bring much computational cost. Nikos proposed the geodesic active regions by adding a region term into the geodesic active

contour model, which combines the region-based segmentation with edge information. The region term is derived by minimizing the negative log-likelihood function of the image, which is obtained by MRF pre-segmentation<sup>[10]</sup>. Although many improvements are achieved by introducing region information to guide the curve deforming, their complex speed form brings big computational cost as well.

Considering both the segmentation quality and computational cost, in this paper we propose an efficient approach to ROI extraction. The deforming curve is modeled as monotonically marching front under a new positive speed field, where a new region speed function is derived by minimizing the ROI energy. Integrating with the region information, the modified speed function has a large propagation range and could even drive the front propagating in low contrast and narrow thin areas. To further improve the segmentation results, a multi-initial Fast Marching algorithm is developed, which permits the user to plant several seed curves as the initial front and evolve them simultaneously. All the seed curves are treated as one complex front driven by the same evolution equation. To greatly reduce the computational cost, a multiscale scheme is presented where the fast passing solution method is used for a passing solution from coarser scale to the finer one<sup>[12]</sup>.

In section 2, Fast Marching method is briefly outlined. In section 3, the curve evolution model is proposed, where a new speed function is introduced by ROI energy-minimizing. In section 4, multi-initial fast marching algorithm is presented and multiscale scheme is described in detail. In section 5, experimental results are presented and compared with those of the other methods. Finally in section 6, conclusions are given.

## 2 Fast Marching Method

Let  $C(p,0)$  be a closed parameterized curve in Euclidean plane  $R^2$ . Let  $C(p,t)$  be the one-parameter family of curves generated by moving  $C(p,0)$  along its normal vector field  $\vec{N}$  with speed  $F$ . The corresponding curve motion equation is given by

$$\begin{cases} \frac{\partial C}{\partial t} = F \cdot \vec{N} \\ C(p,0) = C_0(p) \end{cases} \quad (1)$$

In particular, for the speed function  $F$  being always positive or negative, the front is marching monotonically. One way to characterize the position of this moving front is to compute the arrival time  $T(x,y)$  of the front as it crosses each point  $(x,y)$ . By embedding the moving front to the level set of time function  $T(x,y)$ , the normal vector  $\vec{N}$  could be given by  $\vec{N} = \frac{\nabla T}{|\nabla T|}$ , The Fast Marching equation is derived as follows<sup>[8]</sup>:

$$T(C(p,t))=t \Rightarrow \nabla T \cdot C_t = 1 \Rightarrow \nabla T \cdot \left( F \cdot \frac{\nabla T}{|\nabla T|} \right) = 1 \Rightarrow F \cdot |\nabla T| = 1 \quad (2)$$

The advantages of this equation representation are that it is both intrinsic and topologically flexible since at any time  $t$ , different topologies of  $C$  can be handled naturally by exploiting the level set  $\{C(p,t) | T(C(p,t)) = t\}$ .

## 3 Region Based Curve Evolution Model

### 3.1 ROI energy and region speed function

Assume that ROI is the region enclosed by the moving front and is corresponding to the class  $O$  in the image  $I$ . Let  $\mu_o(I(x,y))$  denote the membership of the pixel belonging to the interesting object class  $O$ . Let

$$P_o(I(x,y)) = \begin{cases} 1, & \text{if } \mu_o(I(x,y)) > 0.5 \\ -\varepsilon, & \text{otherwise} \end{cases} \quad (3)$$

where  $\varepsilon \rightarrow 0^+$  is a small positive constant. We define the ROI energy as follows:

$$E_{ROI} = -\iint_{ROI} P_o(I(x,y)) dx dy \quad (4)$$

A direct explanation of (4) is that ROI should include as much as possible pixels that belong to the class  $O$ .

By using the Green theorem and the variational method, we could derive the corresponding curve evolution equation as follows:

$$\frac{\partial C}{\partial t} = -P_o(I) \cdot \vec{N}_{in} = P_o(I) \cdot \vec{N} \quad (5)$$

where  $\vec{N}$  is the outward normal vector.

From Eq.(5), we could conclude that if a pixel belongs to the class  $O$ , the region force  $P_o(I(x,y)) \cdot \vec{N}$  aims at expanding the front curve to include this pixel; otherwise, it aims at shrinking the front to exclude this pixel.

For many medical images, the gray values constitute an adequate statistic to distinguish one region from another. Therefore, histogram based Deterministic annealing EM (DAEM) algorithm is performed for initial segmentation to provide region information, avoiding trapping into local extrema. Let  $U=[u(l,k)]$  ( $l=0, \dots, 255$ ;  $k=1, \dots, K$ ), where  $u(l,k)$  denotes the membership of the gray level  $l$  belonging to the  $k$ -th class and  $K$  is the number of classes. Then  $\mu_o(I) = u(I(:, :), O)$ . The ROI class  $O$  could be simply determined by choosing several pixels in this region.

### 3.2 Modified speed function

Malladi in Ref.[8] proposes an image based speed function:

$$g_I = e^{-\alpha |\nabla G_\sigma * I|}, \quad \alpha > 0 \quad (6)$$

that could stop the front in the vicinity of the ROI boundary. However, this only edge based speed is too weak to propagate the front in low contrast and narrow thin areas. To address this problem, improvements have been exploited, but this may bring expensive computational cost. By considering both the segmentation quality and computational cost, we introduce the ROI information to the model by integrating the new region speed function  $P_o(I)$  with the edge speed function  $g_I$ . The modified speed function is given by

$$F_{modi} = w_R \cdot P_o(I) + w_E \cdot g_I \quad (7)$$

The corresponding curve evolution equation is

$$\frac{\partial C}{\partial t} = F_{modi} \cdot \vec{N} = w_R \cdot P_o(I) \cdot \vec{N} + w_E \cdot g_I \cdot \vec{N} \quad (8)$$

where  $w_R, w_E \in (0,1]$  are constants weighting the effects of region based speed term and edge based speed term respectively.

If we choose  $\varepsilon = \min\{w_E \cdot g_I / w_R\}$ , the modified speed function  $F_{modi} = w_R \cdot P_o(I) + w_E \cdot g_I$  is always positive. The corresponding Fast Marching equation is given by

$$F_{modi} \cdot |\nabla T| = 1 \quad (9)$$

The modified speed fuses both region and edge information that has a large propagation range, even at weak boundaries, it can provide a proper speed to propagate the front.

## 4 Numerical Implementation

### 4.1 Multi-initial fast marching algorithm

Equation (8) can be implemented by the classical Fast Marching algorithm<sup>[8]</sup>. However, monotonically marching front may leak out of the weak boundary too earlier to arrive at the desired ROI boundary. To address this problem, we develop the multi-initial Fast Marching algorithm that permits the user to plant seed curves as the initial front and evolve them simultaneously, which could perform the selective growth that may further improve the segmentation results and reduce the computational cost. Moreover, we perform the algorithm on multiscale space where the solution on the coarser scale is used to determine the initial front condition on the finer scale that could significantly reduce the computational cost and speed up the convergence rate.

The multi-initial Fast Marching algorithm is given as follows:

#### 1> Initialization

Plant several seed curves in the ROI region;

Let initial front be the set of the pixels on all the seed curves;

*Alive pixel:*

The **front** pixels constitute the *alive* pixels. If we want the front to propagate outward, also tag as *alive* pixels in the interior of every seed curve; Assign *alive* pixels zero crossing time  $T_{alive}(i, j) = 0$ ;

*Trial pixel:*

For each front pixels, the first-order neighborhood pixels are examined. If they are not labeled as *alive*, then they become trial pixels with crossing time  $T_{trial}(i, j) = 1/F_{mod_i}(i, j)$ ;

*Faraway Pixel:*

All other pixels are initialized as faraway with a crossing time  $T_{faraway}(i, j) = \infty$ ;

#### 2> Marching Forward

While(not satisfy stop criterion)

Let  $A$  be the *trial* pixel with the smallest  $T$  value;

Add the pixel  $A$  to *alive* set and remove it from *trial* set ;

Tag as *trial* all neighbors of  $A$  that are not *alive*. If the neighbor is in *faraway*, remove, and add to the *trial* with initial crossing time  $T(i, j) = 1/F_{mod_i}(i, j)$ ;

Recompute the value of  $T$  at all *trial* neighbors of  $A$  according to Eq.(9);

End

An efficient technique for fast locating the grid pixel with the smallest  $T$  in the narrow band is to use a variation on the heap-sort algorithm, resulting in only  $O(N \log N)$  computational expense<sup>[8]</sup>.

### 4.2 Multiscale scheme

The multiscale level set approach uses the solution on the coarser scale to determine the initial front condition on the finer scale, which could reduce significantly the computational cost and speed up greatly the convergence rate.

Let  $I_0, I_1, \dots, I_J$  be a set of multiscale image set.  $I_J$  represents the coarsest scale image and  $I_0$  the original image. The front propagation on  $I_0$  is given by

$$\begin{cases} F_{I_0} \cdot |\nabla T| = 1 \\ T(\cdot, 0) = T_0(\cdot) \end{cases} \quad (10)$$

The solution of (10) is obtained by performing the following level set evolution equations from coarse to fine:

$$F_{I_j} \cdot |\nabla T| = 1 \quad \text{given the initial } T(\cdot, 0) \quad (11)$$

$$\begin{cases} F_{I_j} \cdot |\nabla T| = 1 & j = J-1, \dots, 1, 0 \\ T(\cdot, 0) & \text{given the initial front condition by the passing solution} \end{cases} \quad (12)$$

In Ref.[12], an efficient approach to passing the solution from the coarser scale to the finer one is presented that could induce a very fast convergence. Borrowed from this approach, a multiscale scheme for numerical implementation is developed. On each scale, the fast marching algorithm is applied to evolve the front, and the solution passed from the coarser scale to the finer one is obtained by the approach proposed in Ref.[12]. The multiscale scheme is described as follows:

Step 1

On scale  $J$ , perform the multi-initial Fast Marching algorithm;

Step 2

For  $j=J-1: -1: 0$

Initialize all pixels *Faraway*; if a point  $(k, l)^{(j+1)}$  on the  $j+1$ th scale is *alive*, then its corresponding

four children  $\begin{bmatrix} (2k, 2l)^{(j)} & (2k, 2l+1)^{(j)} \\ (2k+1, 2l)^{(j)} & (2k+1, 2l+1)^{(j)} \end{bmatrix}$  on the  $j$ th scale are also “*alive*”;

Tag as *trial* all neighbors of *alive* pixels that are *faraway*;

Perform Marching Forward on the  $j$ -th scale.

End

## 5 Experiment

To demonstrate the efficiency of our approach, the proposed curve evolution Eq.(8) for ROI extraction by the multi-initial fast marching algorithm is compared with the other methods:

Method 1: ROI extraction based on the only edge based curve evolution<sup>[8]</sup>:

$$\frac{\partial C}{\partial t} = g \cdot \vec{N} \quad (13)$$

Method 2: ROI extraction by geodesic active contours equation<sup>[13]</sup>:

$$\frac{\partial C}{\partial t} = g(c_1 + c_2 \kappa) \cdot \vec{N} - (\nabla g \cdot \vec{N}) \cdot \vec{N} \quad (14)$$

Method 3: Geodesic active region equation proposed by Nikos<sup>[10]</sup>:

$$\frac{\partial C}{\partial t} = (1 - \beta) \cdot [g(c_1 + c_2 \kappa) \cdot \vec{N} - (\nabla g \cdot \vec{N}) \cdot \vec{N}] + \beta \cdot \frac{\log P_B(I(x, y))}{\log P_A(I(x, y))} \cdot \vec{N} \quad (15)$$

Method 4: Fully global approach proposed by Yezzi<sup>[11]</sup>:

$$\frac{\partial C}{\partial t} = (u - v) \cdot \left( \frac{I - u}{A_u} + \frac{I - v}{A_v} \right) \cdot \vec{N} - c \cdot \kappa \cdot \vec{N} \quad (16)$$

where  $g$  is a monotonically decreasing function such that  $g(r) \rightarrow 0$  as  $r \rightarrow \infty$  and  $g(0) = 1$ , and  $\vec{N}$  represents the outward normal vector in Eqs.(13) and (16) whereas inward normal vector in Eqs.(14) and (15).  $c_1, c_2, c$  and  $\beta$  are constants.  $P_A(I(x, y))$  and  $P_B(I(x, y))$  are the joint probability of the image with respect to two class hypotheses  $A$  and  $B$  respectively.  $u$  and  $v$  are the average intensity inside and outside the deforming curve. The common choice of  $g$  is given by Eq.(6).

The numerical implementation of Eq.(8) is given by the proposed multiscale algorithm developed in section 4.2 where the decomposition scale  $J = 1$ . Equation (13) is given by the multi-initial fast marching algorithm. Due to the complex speed function form, the corresponding level set evolution equations of (14)~(16) should be implemented by Hermes algorithm or by the more expensive narrow band method<sup>[9,10]</sup>.

In the following experiments, we choose  $\alpha = 0.2$ .  $c_1 = -1$ ,  $c_2 = 0.05$ ;  $c = 0.05$ ;  $\beta = 0.7$ . The ratio of  $w_R$  and  $w_E$  is recommended that it should be larger for low contrast image or images with many narrow thin branches as the region information is more reliable than the edge information there. The ROI class  $O$ , the class numbers  $K$  used in fuzzy cluster, and the values of  $w_E$  and  $w_R$  for each case are given in Table 1.

**Table 1** Parameters for each case

Fig No.	1	2	3	4	5	6	7	8	9
$w_R$	1.0	0.9	1.0	0.9	Given in each group	1.0	0.9	0.9	1.0
$w_E$	0.2	0.1	0.2	0.2		0.2	0.2	0.2	0.2
Interesting class $O$	Three tumors	Top tumor	Right tumor	DSA Vessels	Vessel branches	Vessel branches	Vessel branches	Vessel branches	bone
$K$	3	5	5	2	2	2	2	2	2

Figures 1~4 are the comparison results. The group (a) provides the results by our approach and the group (b) shows the results by Method 1~Method 4 respectively. In group (a), the multiscale solution is provided where the first three columns show the segmentation results on the coarser scale; the fourth column shows the passed solution and the fifth column shows the final segmentation results on the finer scale. In group (b), the first column shows the initial seed curves, the second and the third columns show the random middle state of the marching front, and the fourth column shows the final front state.

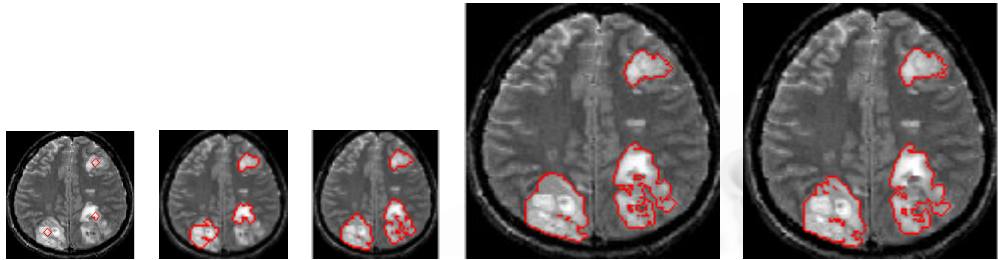
Figure 1 is a sarcoma pathological brain MR image, where three tumors are to be extracted. In the initial state, three seed curves are planted in the tumor areas, therefore tumors can be extracted at one time. It can be seen from Fig.1(b) that because of the low contrast and complex gradient of the ROI, the only edge based speed misleads the deforming behavior. However, the results of Fig.1(a) are very promising, which shows that the modified speed function integrating region information has a large propagation range in low contrast area.

Figure 2 is a meningioma pathological brain MR image where the tumor area is the ROI. In this experiment, we compare the effect of the proposed region speed term with the advection speed term in geodesic active contours. In Fig.2(a), the narrow thin area on the top could be extract. In Fig.2(b), Method 2 fails in extracting the thin area due to the low gradient information. Experimental results show that compared with the advection term, the region force has a larger attraction ability to guide the curve deforming in thin areas.

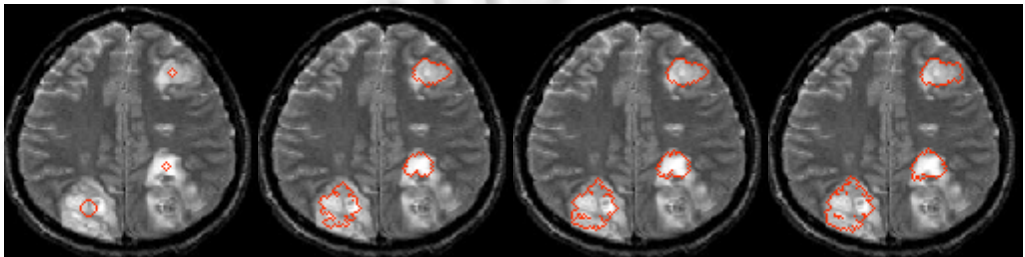
Figure 3 is a Metastatic bronchogenic carcinoma pathological brain MR image where the tumor in the right is the ROI. The result given by our approach is slightly different from that of Nikos's geodesic active region method. However, the pre-segmentation map of Method 3 comes from the MRF-based segmentation, and the region information used for curve evolution involves two terms:  $P_A(I(x, y))$  and  $P_B(I(x, y))$ , corresponding to the joint probability of the image with respect to two class hypotheses. Our region information only involves the ROI class  $o$  hypothesis. In addition, the computational cost of multi-initial fast Marching algorithm used in our approach is

$O(N\log N)$  whereas the Hermes algorithm used for Method 3 is more expensive.

Figure 4 is a DSA blood vessel. The result given by our approach is almost the same as that of Method 4. However, the numerical implementation of Yezzi's equation needs to use the narrow band algorithm that is far more expensive than the fast marching algorithm. Moreover, the statistics of the average intensity  $u$  and  $v$  are variable with the deforming curve, thus continuously computing of these statistics is needed during the curve evolution which brings more computational cost.

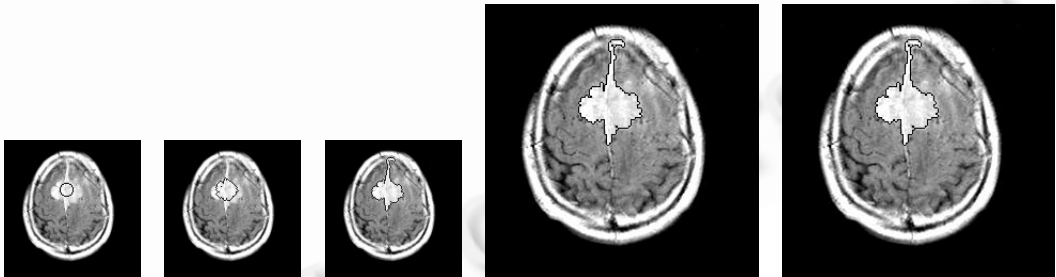


(a) Sarcoma tumors extraction by the proposed approach

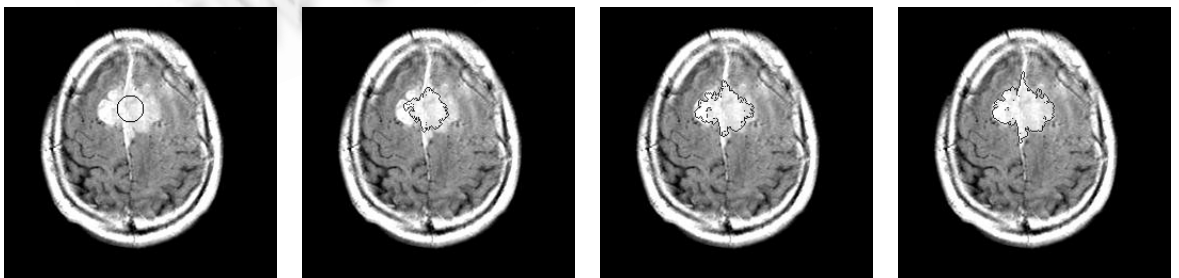


(b) Sarcoma tumors extraction by Method 1: The only edge based approach

Fig.1

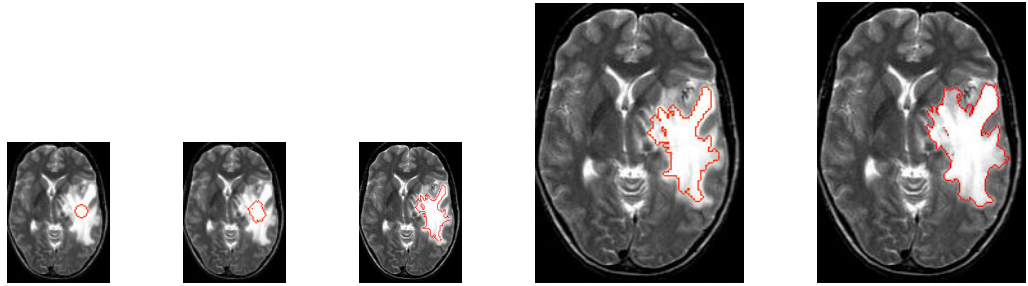


(a) Meningioma tumor extraction by the proposed approach

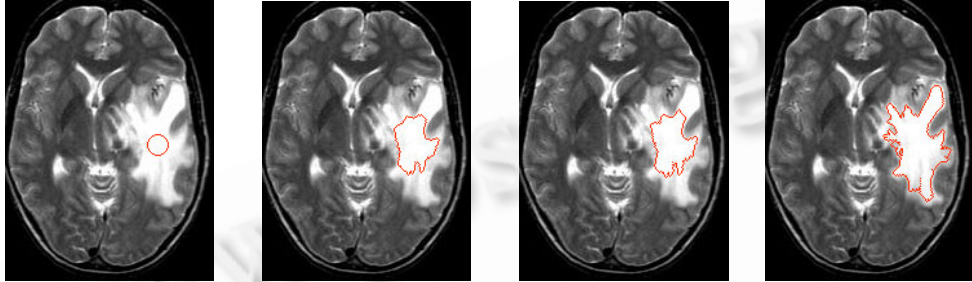


(b) Meningioma tumor extraction by Method 2: Geodesic active contours

Fig.2

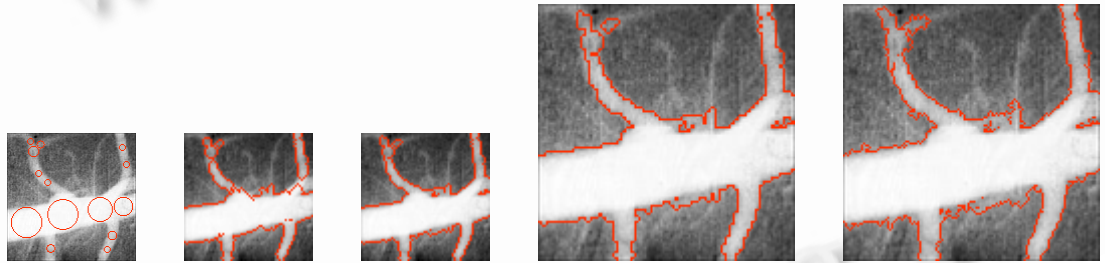


(a) Carcinoma tumor extraction by our approach

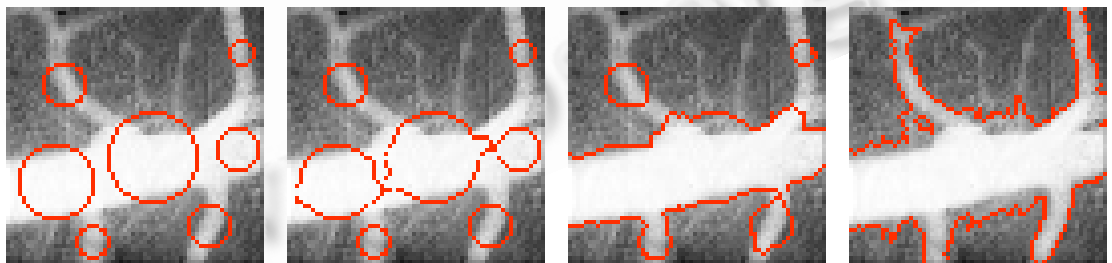


(b) Carcinoma tumor extraction by Method 3: Geodesic active regions approach

Fig.3



(a) DSA vessel extraction by the proposed approach



(b) DSA vessel extraction by Method 4: Fully global approach

Fig.4

Considering both the computing cost and the segmentation results, our approach performs better than the other methods in that it runs faster and could locate the curve in the desired boundary as well, which is suitable for real time medical image ROI extraction.

In our approach, choosing parameters of  $w_R$  and  $w_E$  is important to guide the curve deforming. Figure 5 shows the impact of different combination of  $w_R$  and  $w_E$  on the pulmonary vessels extraction. The obtained image is preprocessed by contrast enhancement, where vessels network is the ROI. From the comparison of the four groups in Fig.5, we can see that increasing the value for  $w_R$  can improve the image segmentation results significantly.

Experimental results show that for low contrast image or images with many narrow thin branches, the larger  $w_R$  could perform better as region information plays a prominent role in guiding the front propagation.

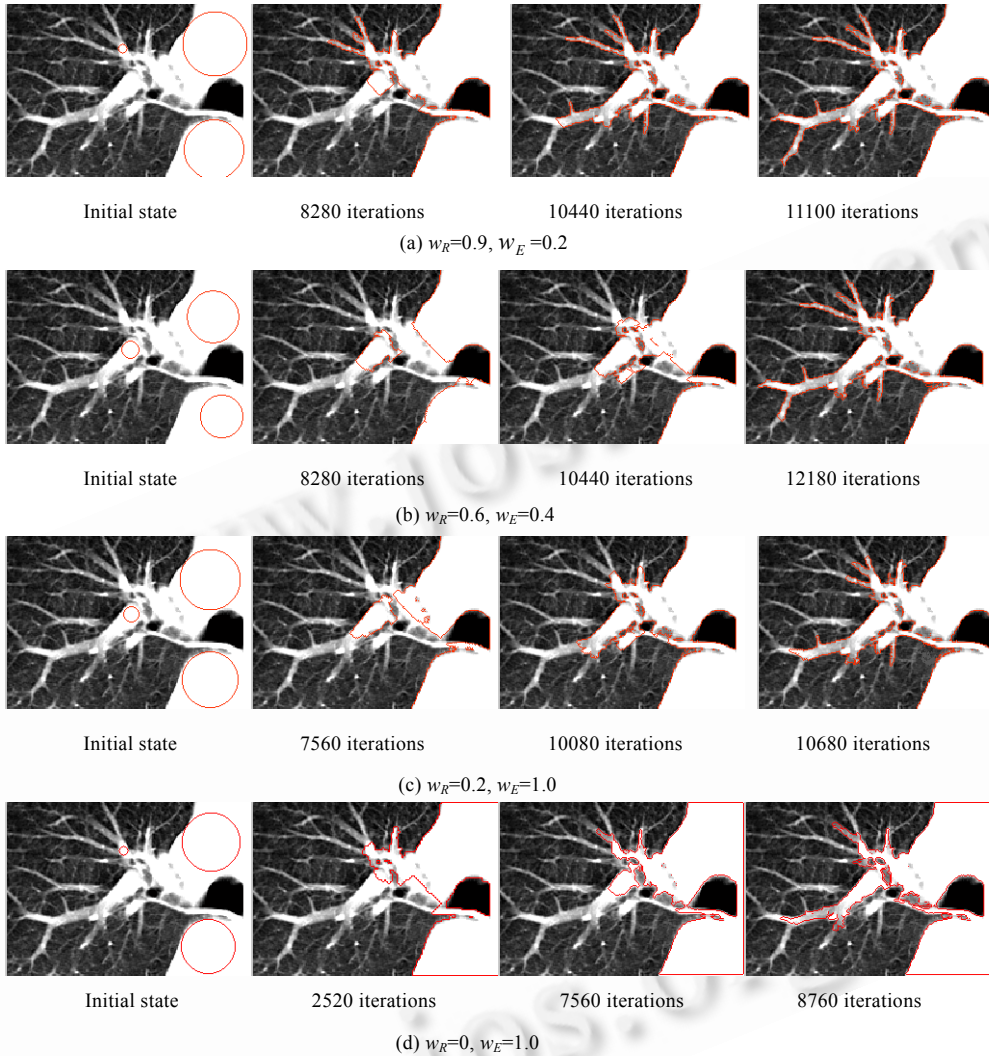


Fig.5 Impact of different combination of  $w_R$  and  $w_E$  on the pulmonary vessels extraction

In the fast marching algorithm, because the front is monotonically marching, too earlier front leaking from the boundary is a serious problem. Multi-initial planting seed curves can help the selective growth of the front that may avoid this problem. Seed curves are recommended to plant in some narrow thin vessels branches or low contrast areas, inducing the front growth. In addition, the interior of every seed curve is alive pixels, which needs not to be updated in the marching processing, therefore planting seed curves may reduce the computational cost. Figure 6 shows the results by our multi-initial fast marching algorithm and the classical fast marching algorithm without multi-initial. The comparison shows that the selective planting seed curves can indeed help on local growth of the front and also reduce the computational cost to some extent.

To further demonstrate the reliability of the proposed approach, experiments on several medical images segmentation are performed. The numerical implementation is given by the proposed multiscale algorithm. Figure 7 is the MR image where the white matter is precisely extracted by our approach. Figure 8 is the pulmonary vessel

selected from CT images. Observation shows that the front stops at the desired vessel boundary, even some small and thin vessel branches, which exhibits much variability, could be located precisely as well. Almost the whole vessels network is extracted by our approach. Figure 9 is a bone image. From the segmentation results, we could see thin bones on the two sides are precisely extracted by our approach.

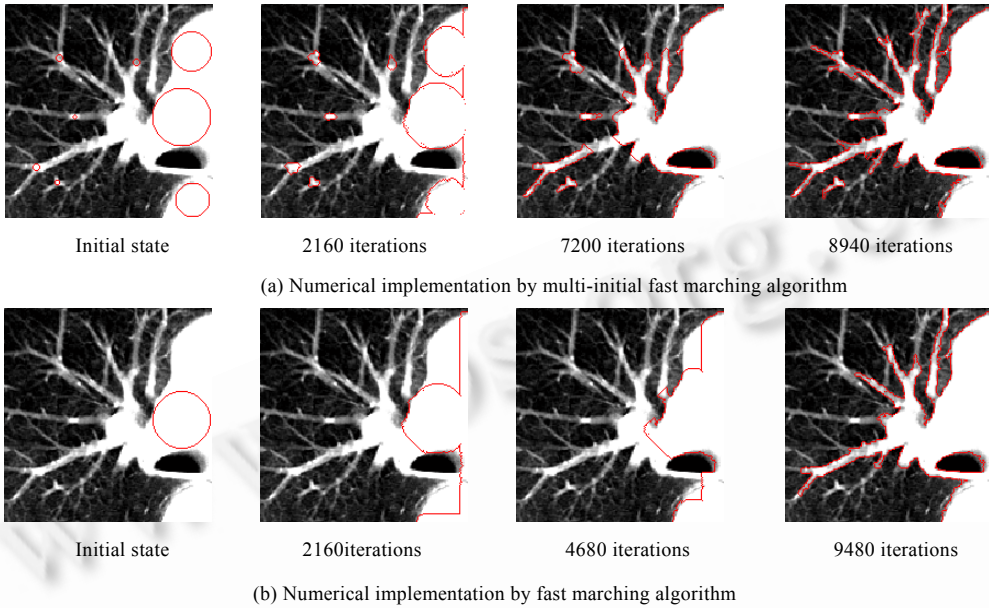


Fig.6

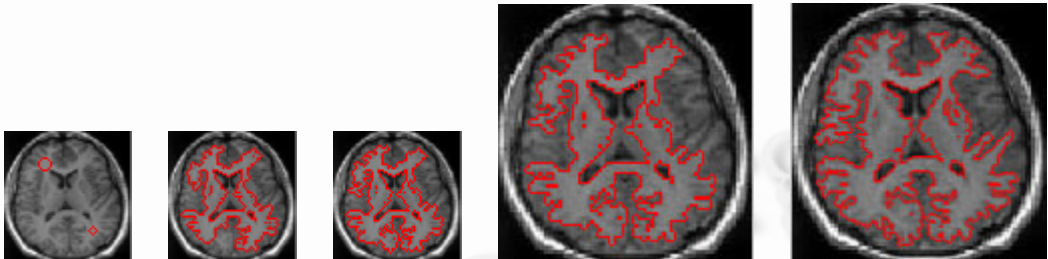


Fig.7 MR white matter extraction by the proposed approach

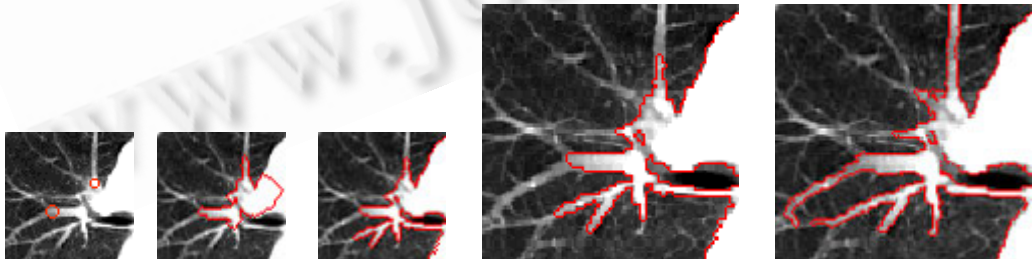


Fig.8 Pulmonary vessel extraction by the proposed approach

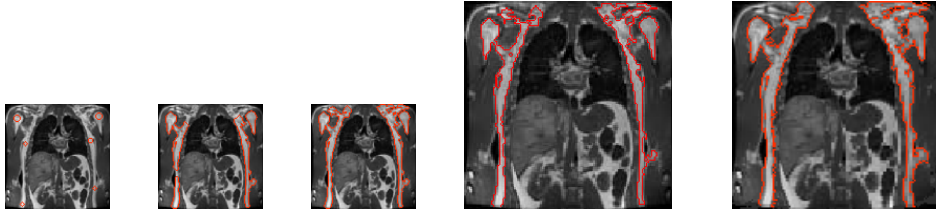


Fig.9 Medical bone image extraction by the proposed approach

## 6 Conclusion

In this paper, an efficient monotonically marching snake integrating ROI information is proposed. Due to the region based speed term, the front could even propagate in low contrast and narrow thin areas. Furthermore, multiscale multi-initial fast marching algorithm is developed for numerical implementation, where the multi-initial scheme can perform the selective growth of the front, thus further reduce the front leaking and the multiscale scheme can greatly reduce the computational cost. Experiments on several medical images are provided and compared with those of the other methods, showing that complex MR tumor and CT pulmonary vessels can be extracted accurately by our approach. Our approach is efficient both in computational cost and segmentation result, and can be applied to medical image segmentation.

## References:

- [1] Lorigo LM, Faugeras OD, Grimson WEL, Keriven R, Kikinis R, Nabavi A, Weston CF. Curves: Curve evolution for vessel segmentation. *Medical Image Analysis*, 2001,5:185–206.
- [2] Kass M, Witkin A, Terzopoulos D. Snakes: Active contour models. *Int'l Conf. on Computer Vision*. 1987. 321–331.
- [3] Chakraborty A, Staib LH, Duncan JS. Deformable boundary finding in medical images by integrating gradient and region information. *IEEE Trans. on Medical Imaging*, 1996,15(6):859–870.
- [4] Ivins J, Porrill J. Constrained active region models for fast tracking in color image sequences. *Image and Vision Computing*, 1998, 72(1):54–71.
- [5] Zhu S, Lee T, Yuille A. Region competition: Unifying snakes, region growing, and Bayes/MDL for multiband image segmentation. *IEEE Int'l Trans. on Pattern Analysis and Machine Intelligence*, 1996,18(9):884–900.
- [6] McInerney T, Terzopoulos D. T-Snakes: Topology adaptive snakes. *Medical Image Analysis*, 2000,4:73–91.
- [7] Sethian JA. *Level Set Methods and Fast Marching Methods: Evolving Interfaces in Computational Geometry, Fluid Mechanics, Computer Vision and Material Science*. Cambridge University Press, 1999.
- [8] Malladi R, Sethian JA. An  $O(N \log N)$  algorithm for shape modeling. In: *Proc. of the National Academy of Sciences*, 1996: 9389–9392.
- [9] Adalsteinsson D, Sethian J. A fast level set method for propagating interfaces. *Journal of Computational Physics*, 1995,118: 269–277.
- [10] Paragios N, Deriche R. Geodesic active regions for motion estimation and tracking. In: *Proc. of the 7th IEEE Int'l Conf. on Computer Vision*. Corfu, 1999. 688–674.
- [11] Jr. Yezzi A, Tsai A, Willsky A. A fully global approach to image segmentation via coupled curve evolution equations. *Journal of Visual Communication and Image Representation*, 2002,13:195–216.
- [12] Zhang HM, Bian ZH, Guo YM, Fei BW, Ye M. An efficient multiscale approach to level set evolution. In: *Proc. of the 25th Silver Anniversary Int'l Conf. of the IEEE Engineering in Medicine and Biology Society*. 2003. 694–697.
- [13] Caselles V, Kimmel R, Sapiro G. Geodesic active contours. *Int'l Journal of Computer Vision*, 1997,22(1):61–79.